

Distributed Backlog-Aware D2D Communication for Heterogeneous IIoT Applications

Hossam Farag*, Čedomir Stefanović* and Mikael Gidlund†

*Department of Electronic Systems, Aalborg University, Denmark

†Department of Information Systems and Technology, Mid Sweden University, Sweden

Email: hmf@es.aau.dk, cs@es.aau.dk, mikael.gidlund@miun.se

Abstract—Delay and Age-of-Information (AoI) are two crucial performance metrics for emerging time-sensitive applications in Industrial Internet of Things (IIoT). In order to achieve optimal performance, studying the inherent interplay between these two parameters in non-trivial task. In this work, we consider a Device-to-Device (D2D)-based heterogeneous IIoT network that supports two types of traffic flows, namely AoI-orientated. First, we introduce a distributed backlog-aware random access protocol that allows the AoI-orientated nodes to opportunistically access the channel based on the queue occupancy of the delay-oriented node. Then, we develop an analytical framework to evaluate the average delay and the average AoI, and formulate an optimization problem to minimize the AoI under a given delay constraint. Finally, we provide numerical results to demonstrate the impact of different network parameters on the performance in terms of the average delay and the average AoI. We also give the numerical solutions of the optimal parameters that minimize the AoI subject to a delay constraint.

Index Terms—Industrial IoT, AoI, D2D communication

I. INTRODUCTION

The emerging technology of Internet of Things (IoT) enables ubiquitous connectivity and innovative services spanning a wide range of applications, such as industrial automation, healthcare and intelligent transportation [1]. The realization of such applications implies the interconnection of a large number of heterogeneous and pervasive IoT devices continuously generating and transmitting sensor data to their respective destinations. According to the Global System for Mobile Communications Association (GSMA), it is expected that the number of connected IoT devices will grow up to 75 billion by 2025 [2]. As a subset of the IoT, Industrial IoT (IIoT) has gained significant attention as a key technology supporting machine type communication for time-sensitive industrial applications [3]. For a vast number of IIoT applications, the field network comprises a high number of sensors and actuators that sense the physical environment and perform appropriate actions, respectively [4]. Different from the conventional star-network configuration with a static sink, Device-to-device (D2D) communications provide a promising transmission paradigm for sensor-actuator pairs which are in propinquity [5]. In such setups, sensors directly transmit data to actuators without involving a central node, resulting in improved throughput and energy efficiency.

Typically, the field network in IIoT applications supports transmissions of heterogeneous traffic flows which are characterized by different performance objectives [6]. In process

monitoring and control scenarios, the distributed sensor nodes either report special events to their corresponding actuators that perform actions in response, or transmit either status updates about a certain process. In the former case, it is essential to maintain low latency communication of event reporting from sensors to actuators in order to avoid production inefficiency or safety-critical situations. An event could be any incident happening, e.g., fire or leakage of gas, that should be delivered to the corresponding actuator within a predefined deadline. In the latter case, the freshness of the status updates is crucial for proper functioning of the system as the actuation decisions are mainly influenced by the freshest information available [7]. For instance, in oil refineries, valve actuators should acquire timely monitoring of oil level to avoid spilling of oil tanks [8]. Classical time-related performance metrics, such as throughput and delay, have a transmitter-side view of the channel and are insufficient to reflect information freshness at the receiver side. Age of Information (AoI) has been proposed to characterize information freshness which measures the time elapsed since the generation of the most recently received packet [9]. Although D2D communication can improve throughput and energy efficiency [10], the high number of deployed sensor-actuator pairs and the uncoordinated channel access pose a challenge on guaranteeing the performance objectives (low latency and low AoI) of heterogeneous traffic streams.

In this work, we consider a D2D-based heterogeneous IIoT network that supports two traffic flows, delay-oriented traffic and AoI-oriented traffic. The delay-oriented traffic is transmitted by a single node and is subject to a predefined delay constraint, while the AoI-oriented traffic is transmitted by a set of nodes distributed according to a stochastic point process. Our contributions in this work can be summarized as follows:

- We introduce a distributed backlog-aware random access protocol, in which the AoI-oriented nodes access the shared channel based on the backlog status of the delay-oriented node.
- Using stochastic geometry, Discrete-Time Markov Chain (DTMC) and queueing theory, we derive closed-form expressions for the average AoI, average delay, and the average queue size of the delay-oriented node, and formulate an optimization problem to minimize the average

AoI under a given delay constraint.

- We evaluate the network performance using numerical results in order to investigate the impact of different network parameters on the average AoI and the average delay.
- We solve the formulated optimization via a 2-D exhaustive search under different network parameters.

II. RELATED WORK

AoI has been receiving a growing attention as a promising metric for time-sensitive applications. Several works were conducted to study and analyze AoI utilizing queuing theory [11], [12]. The AoI minimization problem has been addressed through different approaches including packet management schemes [13], [14], adjusting sampling rate [9] and introducing packet deadlines [15]. The queuing analysis in these works considers only the temporal traffic dynamics associated with the transmitters and receivers based on the assumption of an error-free channel, i.e., without considering transmission failures due to interference and collisions that are inevitable in the industrial environment. In [16]–[19], the authors introduced a number of scheduling protocols with the goal to minimize the average AoI considering wireless networks with unreliable channels. All these works are based on a centralized scheduling policy which is not applicable to the D2D communication scenario in IIoT, as it would incur high communication overhead and cannot scale with the network size.

The main research on scheduling in wireless D2D networks focuses on the analysis and optimization of resource allocation [20], traffic density [21], or user fairness [22], however, there are few works that focus on the study and minimization of AoI. The authors in [23] statistically analyzed the peak AoI and the conditional success probability in a D2D communication scenario under preemptive and non-preemptive queues. Based on a stochastic geometry approach, the authors in [24] proposed a distributed scheduling policy that utilizes local observations, encapsulated in the concept of stopping sets to make scheduling decisions that minimize the network-wide average AoI. The work in [25] introduced a joint optimization problem of the transmit probability and transmit power to maximize the energy efficiency of a covert D2D communication under AoI constraint. The authors in [26] proposed an age-aware scheduling algorithm where edge controllers assist each D2D node to select a proper resource block and transmit power level to satisfy the AoI constraint. All these works consider that the network supports only a single traffic flow, which is age-oriented traffic and aim to minimize the average AoI without considering the coexistence of other traffic flows. The works in [27], [28] proposed scheduling policies to optimize the AoI while satisfying throughput constraints. The authors in [29] proposed a link scheduling policy for a joint optimization of AoI and throughput based on a deep learning approach. These works assume that, at each timeslot, the same user transmit either AoI-oriented packet or a throughput-oriented packet. The works in [30], [31] study the AoI-delay

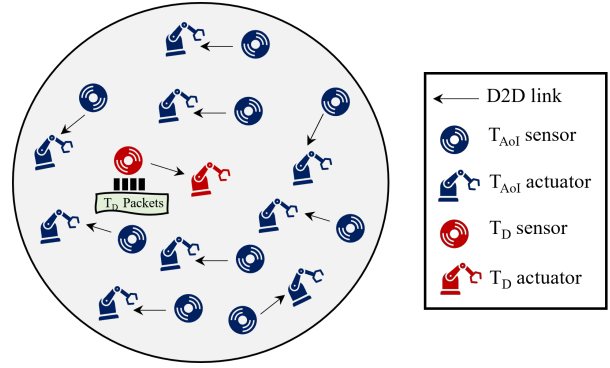


Fig. 1. The network topology with multiple T_{AoI} pairs and a single T_D pair distributed in a circular region \mathcal{C} with a radius R .

tradeoff for multi-server queuing systems considering error-free transmissions which is not applicable to real IIoT systems. In [32], the authors studied the delay and AoI violation probabilities considering finite-block length packets under noisy channels, however, the study was conducted separately for the two parameters.

III. SYSTEM MODEL

A. Network Topology and Communication Model

We consider a heterogeneous IIoT network comprising a set of sensor-actuators (D2D) pairs that are randomly distributed in a circular region \mathcal{C} with a radius R as depicted in Fig. 1. The network supports two traffic flows, namely AoI-sensitive flow (T_{AoI}) and delay-sensitive flow (T_D). The T_{AoI} traffic represent the status updates of an underlying time-varying process, where the T_D traffic denotes event reporting about a certain incident.

In our model, we consider a single D2D pair for transmitting the T_D traffic which characterized by a strict delay performance. The T_D transmitter is fixed in predefined location where the T_D receiver is located at the origin of considered network region with a distance d_D . The T_D transmitter has an infinite output queue where the arrival process of the T_D packets follows a Poisson process with average rate λ_D packets/slot, which captures the scenario where such traffic can be triggered by the occurrence of some random incident [33]. The T_D packets are transmitted in First-Come-First-Served (FCFS) basis, and a packet is removed from the buffer if it is successfully transmitted, which is acknowledged by the T_D receiver through an ACK feedback. If no ACK is received within a predefined timeout, the packet is retransmitted. We assume that the ACK transmission is instantaneous and error-free, which is common assumption in the literature [34].

Further, we consider a set of T_{AoI} transmitters randomly scattered according to a homogeneous Poisson Point Process (PPP) ϕ_A with spatial density λ_A , with $\phi_A = \{x_i = \mathbb{R}^2, \forall i \in \mathbb{N}^+, i \geq 1\}$ [35], where x_i is the location of the i -th T_{AoI} transmitter. Each T_{AoI} transmitter has a dedicated receiver which is located at a distance d_A in a random orientation. The T_{AoI} nodes report status updates following the generate-at will

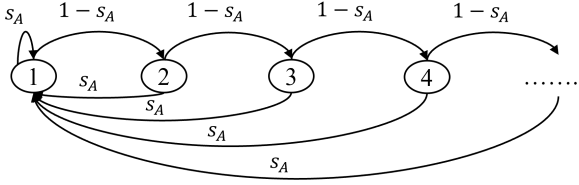


Fig. 2. The DTMC model representing the evaluation of the AoI of the T_{AoI} traffic.

model [9], [36], i.e., the T_{AoI} transmitter is activated with a certain probability, and once becoming active, it samples a fresh packet and transmits it to the T_{AoI} receiver¹. After a transmission attempt, the T_{AoI} discards the packet regardless it is a successful or failed attempt².

The network operates in a time-slotted fashion where the generation and the transmission of a packet is aligned with the boundary of a timeslot and a transmission attempt takes a constant time, which is assumed to be equal to the duration of one timeslot. The T_D transmitter freely access the channel as long as there are packets in its queue. The communication between each D2D pair is performed via a shared communication channel in a slotted ALOHA-like access using a slot-access probability that is subject to optimization. In other words, in every slot there is a random number of interfering users that are active, comprising the T_D and/or the activated T_{AoI} transmitters. The collisions among simultaneously active users are not necessarily destructive, due to the capture effect [39]. In that sense, a packet is decoded successfully at the end of a timeslot when the Signal-to-Interference plus-Noise ratio (SINR) at the corresponding receiver exceeds the capture ratio β . The received SINR at an arbitrary receiving node i is given as

$$\text{SINR}_i = \frac{P_i |h_{i,i}|^2 d_{i,i}^{-\alpha}}{\sigma^2 + \sum_{j \in \mathcal{K} \setminus \{i\}} P_j |h_{j,i}|^2 d_{j,i}^{-\alpha}}, \quad (1)$$

where P_i is the transmitting power of node i , $h_{j,i}$ represents the Rayleigh fading of the channel between the transmitter j and the receiver i with $h_{j,i} \sim \mathcal{CN}(0, 1)$, $d_{j,i}$ is the distance between the transmitter j and the receiver i , α is the path loss exponent, \mathcal{K} is the set of transmitting nodes at the same timeslot and σ^2 denotes additive white Gaussian noise (AWGN) power.

B. Analysis of the Average AoI and the average Delay

In this section, we analyze the Average AoI of the T_{AoI} traffic considering that the status updates from all T_{AoI} nodes are equally important, and without loss of generality, we

¹The generate-at-will model is commonly used for optimal AoI performance as it avoids unnecessary staleness to the sampled information due to queuing [9], [36]–[38]. However, our analysis can be extended to other arrival models.

²This scenario is based on the fact that retransmitting a stale packet might be useless for the receiver. In that sense, it would be better to transmit a fresh status update about the underlying industrial process instead of consuming the communication resources for retransmitting outdated information. Adopting retransmission-aided approach is out of the scope of this paper and left as a future work.

evaluate the average AoI at an arbitrary T_{AoI} receiver in discrete time. In our model, the AoI represents the number of time slots elapsed since the last received T_{AoI} packet was generated. If $\Delta(t)$ denotes the AoI at the end of time slot t , then we have

$$\Delta(t+1) = \begin{cases} \Delta(t) + 1 & \text{unsuccessful transmission} \\ 1 & \text{successful transmission.} \end{cases} \quad (2)$$

Fig. 2 shows the Discrete-Time Markov Chain (DTMC) model of the AoI corresponds to an arbitrary T_{AoI} node where each state represents the value of the AoI at the tagged T_{AoI} receiver. The DTMC transits from any state j to 1 only upon a successful reception of a T_{AoI} packet, otherwise it transits to state $j+1$. Let X_t represent the value of $\Delta(t)$ at time slot t , then the transition probability from state j to state k is $P_{jk} = \Pr(X_{t+1} = k | X_t = j)$, and the transition matrix \mathbf{P}_{AoI} is written as

$$\mathbf{P}_{AoI} = \begin{bmatrix} s_A & 1-s_A & 0 & 0 & \dots \\ s_A & 0 & 1-s_A & 0 & \dots \\ \vdots & \vdots & \vdots & \ddots & \ddots \end{bmatrix}, \quad (3)$$

where s_A denotes the average successful update probability per timeslot, which is defined as the probability that a T_{AoI} is delivered successfully to its corresponding receiver node. The row vector $\boldsymbol{\pi}_{AoI} = [\pi_1, \pi_2, \dots, \pi_{l-1}, \pi_l, \dots]$ represents the steady-state probability vector of the DTMC in Fig. 2, where $\pi_l = \lim_{t \rightarrow +\infty} \Pr(X_t = l)$ denotes the probability that the AoI is equal to n at the steady state.

Using the set of equations $\boldsymbol{\pi}_{AoI} \mathbf{P}_D = \boldsymbol{\pi}_{AoI}$ and $\sum_l \pi_l = 1$, π_l is obtained as

$$\pi_l = s_A (1-s_A)^{(l-1)}, \quad \forall l. \quad (4)$$

Accordingly, the average AoI $\bar{\Delta}$ is calculated as

$$\begin{aligned} \bar{\Delta} &= \sum_{l=1}^{\infty} \pi_l l = \sum_{l=1}^{\infty} l s_A (1-s_A)^{(l-1)} \\ &= \frac{s_A}{1-s_A} \sum_{l=1}^{\infty} l (1-s_A)^l. \end{aligned} \quad (5)$$

Since we have $s_A < 1$, (5) can be rewritten as

$$\bar{\Delta} = \frac{s_A}{1-s_A} \frac{1-s_A}{s_A^2} = \frac{1}{s_A}. \quad (6)$$

However, the average AoI cannot account for extreme AoI events occurring with very low probabilities. As mentioned in Section I, the received updates of the T_{AoI} traffic are used for control and actuation actions, which implies certain requirements on tolerated values of AoI. In that context, we also analyze the AoI violation probability, which is the probability that the AoI exceeds a certain constraint. Denote c as the target AoI constraint, then we can express the AoI violation probability as

$$\begin{aligned} \Pr(\Delta > c) &= 1 - \Pr(\Delta \leq c) = 1 - \sum_{l=1}^c \pi_l \\ &= 1 - \frac{s_A}{1-s_A} \sum_{l=1}^c (1-s_A)^l \stackrel{(b)}{=} (1-s_A)^c, \end{aligned} \quad (7)$$

where (b) is obtained by using $\sum_{i=0}^y x^i = \frac{x^{y+1}-1}{x-1}$ with $x \neq 1$.

We define the average delay D_{avg} of a T_D packet as the time elapsed from the instant the packet was generated until it is successfully delivered to its destination. Therefore, D_{avg} consists of the queueing time of the packet T_D packet and its transmission time. According to Little's law [40], the queueing time is calculated as $\frac{Q_{\text{avg}}}{\lambda_D}$, where Q_{avg} denotes the average queue size of the T_D source. Then, the average delay D_{avg} can be expressed as

$$D_{\text{avg}} = \frac{Q_{\text{avg}}}{\lambda_D} + \frac{1}{s_D}, \quad (8)$$

where s_D is the average probability of a successful transmission of a T_D packet per timeslot (average service probability), which is inversely proportional to the transmission time component of D_{avg} [41]. As we can see from (6) and (8), $\bar{\Delta}$ and D_{avg} depend on the values s_A , s_D and Q_{avg} . In the next sections, we derive the expressions of s_A , s_D and Q_{avg} based on our proposed distributed backlog-aware channel access.

IV. ANALYSIS OF THE PROPOSED DISTRIBUTED BACKLOG-AWARE CHANNEL ACCESS

In the conventional slotted Aloha-based D2D communication, all nodes compete blindly and equally to transmit their data to their respective receivers via the shared channel. For a network with dense T_{AoI} links (which is the scenario of our considered network model), this means that the T_D node will have a low chance to gain access to the channel. This in turn results in a congestion problem where the buffered T_D packets suffers from an extended queueing time and a poor delay performance. However, such performance would be unacceptable in IIoT applications where safety-critical events (T_D traffic), such as fire detection or gas leakage, must be reported with very low delay in order to perform the appropriate actuation in response.

On the other hand, low AoI is required for the T_{AoI} traffic in order maintain fresh knowledge of the underlying industrial process. In that case, it is inefficient to force the T_{AoI} nodes to remain totally silent when the T_D node is active, in particular as the channel offers a possibility for capture effect to take place. In this regard, we propose a backlog-aware channel access to achieve a proper delay-AoI tradeoff in dense IIoT networks. In our proposed scheme, the T_D node transmits a packet in each timeslot as long as it has a non-empty queue, while the T_{AoI} nodes access the channel in an opportunistic, slotted ALOHA fashion, with the slote-access probability optimized according to the status of the queue size of the T_D node. Denoting Q as the random variable representing the queue size of the T_D node, the introduced access model is defined by the following cases.

Case 1: Empty Queue ($Q = 0$)

When the queue of the T_D node is empty, i.e. $Q = 0$, the T_{AoI} nodes access the channel with a probability p_1 . Let ϕ_{A_0} represent the locations of the active T_{AoI} transmitters when the T_D node is silent. Leveraging the thinning property

of Poisson processes [42], ϕ_{A_0} follows a homogeneous PPP with intensity $p_1 \lambda_A$ and we have $\mathcal{K} = \phi_{A_0}$. According to Slivnyak's theorem [42] and without loss of generality, the following analysis focuses on a typical active T_{AoI} pair. For the considered channel model and conditioned on the spatial realization ϕ_{A_0} , the successful decoding probability p_{A_0} at the tagged T_{AoI} receiver when $Q = 0$ is obtained as

$$\begin{aligned} p_{A_0} &= \Pr(\text{SINR}_i > \beta \mid \mathcal{K} = \phi_{A_0}) \\ &= \Pr\left(\frac{P_2 |h_{i,i}|^2 d_A^{-\alpha}}{\sigma^2 + \sum_{j \in \phi_{A_0} \setminus \{i\}} P_2 |h_{j,i}|^2 d_{j,i}^{-\alpha}} > \beta\right) \\ &\stackrel{(a)}{=} \exp\left(-\frac{\pi p_1 \lambda_A d_A^2 \beta^{\frac{2}{\alpha}}}{\text{sinc}(\frac{2}{\alpha})}\right) \exp\left(-\frac{\beta \sigma^2 d_A^\alpha}{P_2}\right), \end{aligned} \quad (9)$$

where P_2 is the transmitting power of the T_{AoI} nodes. The result in (a) follows by leveraging the Rayleigh distribution of the channel gain, i.e., $|h_{j,i}|^2 \sim \exp(1)$ and the the probability generating functional (PGFL) of the PPP [35].

Case 2: Moderate Backlog ($1 \leq Q \leq M$)

We denote M as the backlog threshold that will determine the activity limit for the T_{AoI} nodes. When the queue is non-empty, the T_D node transmits in each timeslot, while the T_{AoI} nodes attempt to access the channel with a probability p_2 . We assume that $p_2 < p_1$, as the T_{AoI} nodes should cause, as well as experience a lower interference level on the channel. Let x_D represent the location of the T_D node and ϕ_{A_1} denote the locations of the active T_{AoI} nodes that follow a homogeneous PPP with intensity $p_2 \lambda_A$. Then we have $\mathcal{K} = \{x_D \cup \phi_{A_1}\}$. In this case, the successful decoding probability p_{D_1} at the T_D receiver, conditioned on the spatial realization ϕ_{A_1} , is given as

$$\begin{aligned} p_{D_1} &= \Pr(\text{SINR}_D > \beta \mid \mathcal{K} = \{x_D \cup \phi_{A_1}\}) \\ &= \Pr\left(\frac{P_1 |h_{D,D}|^2 d_D^{-\alpha}}{\sigma^2 + \sum_{j \in \phi_{A_1}} P_2 |h_{j,D}|^2 d_{j,D}^{-\alpha}} > \beta\right) \\ &= \exp\left(-\frac{\pi p_2 \lambda_A d_D^2 \left(\beta \frac{P_2}{P_1}\right)^{\frac{2}{\alpha}}}{\text{sinc}(\frac{2}{\alpha})}\right) \exp\left(-\frac{\beta \sigma^2 d_D^\alpha}{P_1}\right). \end{aligned} \quad (10)$$

For the active T_{AoI} nodes, we derive the successful decoding probability at an arbitrary T_{AoI} receiver using the following proposition.

Proposition 1: When $1 \leq Q \leq M$, the successful decoding probability p_{A_1} at an arbitrary T_{AoI} node is given by

$$p_{A_1} = \exp\left(-\frac{\pi p_2 \lambda_A d_A^2 \beta^{\frac{2}{\alpha}}}{\text{sinc}(\frac{2}{\alpha})}\right) \frac{\exp\left(-\frac{\beta \sigma^2 d_A^\alpha}{P_2}\right)}{1 + \frac{d_A^2}{\mathbb{E}[d_{D,i}^2]} \left(\beta \frac{P_1}{P_2}\right)^{\frac{2}{\alpha}}} \quad (11)$$

where we have

$$\mathbb{E}[d_{D,i}] = \int_0^{2\pi} \frac{1}{2\pi} \int_0^R \frac{2r}{R^2} \sqrt{r^2 + d_{D,0}^2 - 2d_0 d_{D,0} \cos \theta} dr d\theta.$$

Proof: See Appendix A.

$$s_A = p_1 \exp \left(-\frac{\pi p_1 \lambda_A d_A^2 \beta \frac{2}{\alpha}}{\text{sinc}(\frac{2}{\alpha})} \right) \exp \left(-\frac{\beta \sigma^2 d_A^\alpha}{P_2} \right) \left(\frac{(p_{D_1} - \lambda_D)(p_{D_0} - \lambda_D)}{p_{D_1} p_{D_0} - \lambda_D p_{D_1} - \lambda_D \left[\frac{\lambda_D (1-p_{D_1})}{(1-\lambda_D) p_{D_1}} \right]^M (p_{D_0} - p_{D_1})} \right) \\ + p_2 \exp \left(-\frac{\pi p_2 \lambda_A d_A^2 \beta \frac{2}{\alpha}}{\text{sinc}(\frac{2}{\alpha})} \right) \frac{\exp \left(-\frac{\beta \sigma^2 d_A^\alpha}{P_2} \right)}{1 + \frac{d_A^2}{\mathbb{E}[d_{D,i}^2]} \left(\beta \frac{P_1}{P_2} \right)^{\frac{2}{\alpha}}} \left(\frac{\lambda_D (1 - \psi^M)(p_{D_0} - \lambda_D)}{p_{D_1} p_{D_0} - \lambda_D p_{D_1} - \lambda_D \psi^M (p_{D_0} - p_{D_1})} \right). \quad (21)$$

$$s_D = \frac{\exp \left(-\frac{\pi p_2 \lambda_A d_D^2 \left(\beta \frac{P_2}{P_1} \right)^{\frac{2}{\alpha}}}{\text{sinc}(\frac{2}{\alpha})} \right) \exp \left(-\frac{\beta \sigma^2 d_D^\alpha}{P_1} \right) \left(\frac{\lambda_D (1 - \psi^M)(p_{D_0} - \lambda_D)}{p_{D_1} p_{D_0} - \lambda_D p_{D_1} - \lambda_D \psi^M (p_{D_0} - p_{D_1})} \right)}{1 - \left(\frac{(p_{D_1} - \lambda_D)(p_{D_0} - \lambda_D)}{p_{D_1} p_{D_0} - \lambda_D p_{D_1} - \lambda_D \left[\frac{\lambda_D (1-p_{D_1})}{(1-\lambda_D) p_{D_1}} \right]^M (p_{D_0} - p_{D_1})} \right)} \\ + \frac{\exp \left(-\frac{\beta \sigma^2 d_D^\alpha}{P_1} \right) \left(\frac{\lambda_D \psi^M (p_{D_1} - \lambda_D)}{p_{D_1} p_{D_0} - \lambda_D p_{D_1} - \lambda_D \psi^M (p_{D_0} - p_{D_1})} \right)}{1 - \left(\frac{(p_{D_1} - \lambda_D)(p_{D_0} - \lambda_D)}{p_{D_1} p_{D_0} - \lambda_D p_{D_1} - \lambda_D \left[\frac{\lambda_D (1-p_{D_1})}{(1-\lambda_D) p_{D_1}} \right]^M (p_{D_0} - p_{D_1})} \right)} \quad (22)$$

the average age Δ , which is equivalent to $p_1^* = \arg \max_{p_1 \in [0,1]} s_A$.

So we have the following optimization problem

$$\min_{p_1} p_1 \exp \left(-\frac{\pi p_1 \lambda_A d_A^2 \beta \frac{2}{\alpha}}{\text{sinc}(\frac{2}{\alpha})} \right) \exp \left(-\frac{\beta \sigma^2 d_A^\alpha}{P_2} \right) \quad (23)$$

subject to $0 < p_1 \leq 1$.

The optimization problem in (23) can be solved via the first-order optimality condition [43], which yields

$$1 - p_1 \frac{\pi \lambda_A d_A^2 \beta \frac{2}{\alpha}}{\text{sinc}(\frac{2}{\alpha})} = 0 \\ \Rightarrow p_1 = \frac{\text{sinc}(\frac{2}{\alpha})}{\pi \lambda_A d_A^2 \beta \frac{2}{\alpha}} \quad (24) \\ p_1^* = \min \left\{ \frac{\text{sinc}(\frac{2}{\alpha})}{\pi \lambda_A d_A^2 \beta \frac{2}{\alpha}}, 1 \right\}.$$

By setting the obtained optimal access probability p_1^* in (13), and by fixing the arrival rate λ_D and the transmission power P_1 , we can see that the average AoI Δ mainly depends on the access probability p_2 and the transmission power P_2 .

Remark 1: The average delay D_{avg} is an independent function of p_1 given a certain value of λ_D . On the other hand, increasing p_2 and/or P_2 would in turn improve Δ for the T_{AoI} nodes but at the cost of increased delay D_{avg} for the T_D node due to the increased level of interference. This is because the probability p_{D_1} is decreased accordingly leading to increased queuing time at the T_D node. Thus, the average delay D_{avg} is an increasing function of p_2 and P_2 .

For a given delay constraint D_{max} of the T_D traffic, there exists an optimal pair (p_2^*, P_2^*) that minimizes the average AoI Δ . Considering the delay constraint D_{max} and the queue stability condition ($\lambda_D < p_{D_0}$) of the T_D node, the optimal

TABLE I
EVALUATION PARAMETERS.

Parameter	Value
λ_A	2×10^{-4}
d_D	100 m
d_A	50 m
R	300 m
α	3
β	0 dB
σ^2	-90 dBm
P_1	100 mW
P_{max}	0.02 mW
D_{max}	5 time slots

pair (p_2^*, P_2^*) lies within a feasible region F_R that can be defined as

$$F_R = \{(p_2, P_2) : D_{avg} < D_{max}, \lambda_D < p_{D_0}\}. \quad (25)$$

In order to find the optimal pair (p_2^*, P_2^*) , we formulate the following optimization problem

$$\min_{(p_2, P_2)} \Delta \\ \text{subject to } D_{avg}(p_2, P_2) < D_{max} \quad (26) \\ 0 < p_2 \leq 1 \\ 0 < P_2 \leq P_{max},$$

where P_{max} denotes the maximum transmission power of the T_{AoI} nodes. Deriving closed form solutions for the optimal values (p_2^*, P_2^*) is a hard problem due to the complexity of the corresponding expressions of s_D , s_A and D_{avg} . Therefore, in the next section we do a numerical analysis of the solution to the optimization problem in (26).

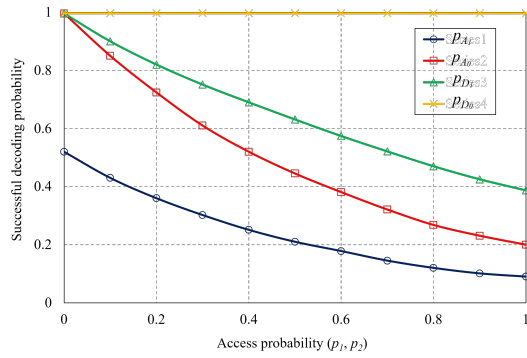


Fig. 4. Evaluation of the successful decoding probabilities with varying p_1 and p_2 with $P_2 = 0.01$ mW.

VI. RESULTS AND DISCUSSION

In this section, we present numerical results to evaluate the performance of the proposed backlog-aware method in terms of the average delay (D_{avg}) and the average AoI (Δ). We also introduce numerical solutions to the optimization problem (26) under different values of λ_D and M . Unless stated otherwise, we adopt the evaluation parameters described in Table I.

Fig. 4 shows the successful decoding probabilities in (9), (10), (11) and (12) as a function of the access probabilities p_1 and p_2 . The value of p_{D0} is independent of the access probabilities p_1 and p_2 , thus showing a constant value of 0.996. The successful decoding probability p_{A0} depends only on p_1 while the values of p_{D1} and p_{A1} depend on p_2 . Increasing p_1 implies higher collision probability between the T_{AoI} nodes, hence decreasing p_{A0} . Also, when the T_D node is active ($1 \leq Q \leq M$), increasing p_1 would in turn decrease both p_{A1} and p_{D1} . In order to satisfy the queue stability condition $\lambda_D < p_{D0}$, we utilize $\lambda_D < 0.996$ for all the following results.

Fig. 5 presents the average AoI Δ versus the access probability p_2 under different values of $\lambda_D \in \{0.2, 0.6\}$ and $M \in \{1, 3\}$. Besides the numerical results obtained from (6), we also plot the simulation results obtained via discrete-time simulations in MATLAB to support our analytical analysis. Each simulation run lasts for 10^4 timeslots, and we plot the average results over 100 runs. First, we can see that the simulation results match well with the numerical results, which validates our analytical analysis presented in Section ****. Moreover, we note that Δ is not a monotonic function of p_2 . At very low values of p_2 , the tagged T_{AoI} node is likely to be inactive for excessive period of time. For a certain values of λ_D and M , the average AoI first decreases as p_2 increases where the tagged T_{AoI} node tends to transmit updates to its corresponding actuator more frequently. However, after a certain value of p_2 , the average AoI at the corresponding actuator starts to significantly increase due to consecutive failed transmission attempts from the tagged source as a result of increased level of contention among the T_{AoI} nodes. We also observe that increasing M would improve the AoI as it implies a higher chance for the T_{AoI} source to be active. For the same M , higher λ_D degrades the AoI performance as the

TABLE II
NUMERICAL SOLUTIONS TO THE OPTIMIZATION PROBLEM IN (26).

λ_D	M	p_2^*	$P_2^*(mW)$	Δ^*
0.2	1	0.275	0.0122	8.22
	3	0.303	0.0185	6.65
	6	0.282	0.0161	6.01
0.6	1	0.145	0.0091	13.28
	3	0.192	0.0132	11.22
	6	0.184	0.0121	10.08
0.8	1	0.125	0.0063	16.81
	3	0.132	0.0072	15.01
	6	0.108	0.0055	14.09

probability $\Pr(Q > M)$ increases, which implies that the T_{AoI} nodes remain silent (*Case 3* in Section IV).

Fig. 6 shows the evaluation of the average delay D_{avg} against p_2 under different values of $\lambda_D \in \{0.2, 0.6, 0.8\}$ and $M \in \{1, 3, 9\}$. For a certain M , we can observe that the average delay increases rapidly as p_2 increases and tends to saturate at a certain point at high values of λ_D , which can be explained as follows. Increasing p_2 will in turn decrease p_{D1} due to the increased interference from the T_{AoI} nodes, which leads to extended average queueing time at the T_D node. When λ_D is high, it is likely that the T_{AoI} nodes remain inactive as the probability $\Pr(Q > M)$ is high, hence the T_D node would probably have interference-free transmission with a stable delay. This also explains the counter-intuitive observation in Fig. 6 where the T_D node may experience a lower delay at high value of λ_D than the one at low value of λ_D . The figure also shows that, for the same λ_D , increasing M degrades the average delay, because the backlog-aware strategy becomes weaker leading to lower s_D and higher D_{avg} accordingly.

Fig. 7 plots the boundary of the feasible region F_R defined in (25) with $\lambda_D \in \{0.2, 0.6\}$ and $M \in \{1, 3\}$. The area below each curve comprises the possible pairs (p_2, P_2) that solve the optimization problem in (26) and satisfy the delay constraint D_{max} . As we can see from the figure, higher M implies narrower F_R where the average delay becomes higher, hence narrowing down the feasible region of (p_2, P_2) that satisfies the delay constraint D_{max} .

In Table II, we present the numerical solutions (p_2^* , P_2^*) to the optimization problem in (26) under different values of λ_D and M and give the minimum achievable average AoI Δ^* . The optimal solutions presented in this table are obtained via a 2-D numerical exhaustive search. As we can see, for the same value of λ_D , the minimum average AoI (Δ^*) can be improved by increasing M as the probability that the T_{AoI} node to be active is increased accordingly, i.e., higher p_2^* . However, higher M increases the average delay as shown by Fig. 6, and tighten the feasible region F_R in order to satisfy the constraint D_{max} . For instance, when $\lambda_D = 0.2$, increasing M from 1 to 3 would improve Δ^* when the p_2^* is increased from 0.275 to 0.303. However, increasing M further to 6 would imply decreasing p_2^* to 0.282 in order to keep p_{D1} sufficiently high to comply with the delay constraint of $D_{max} = 5$ timeslots. In addition, for a given value of M , the optimal access probability p_2^* and

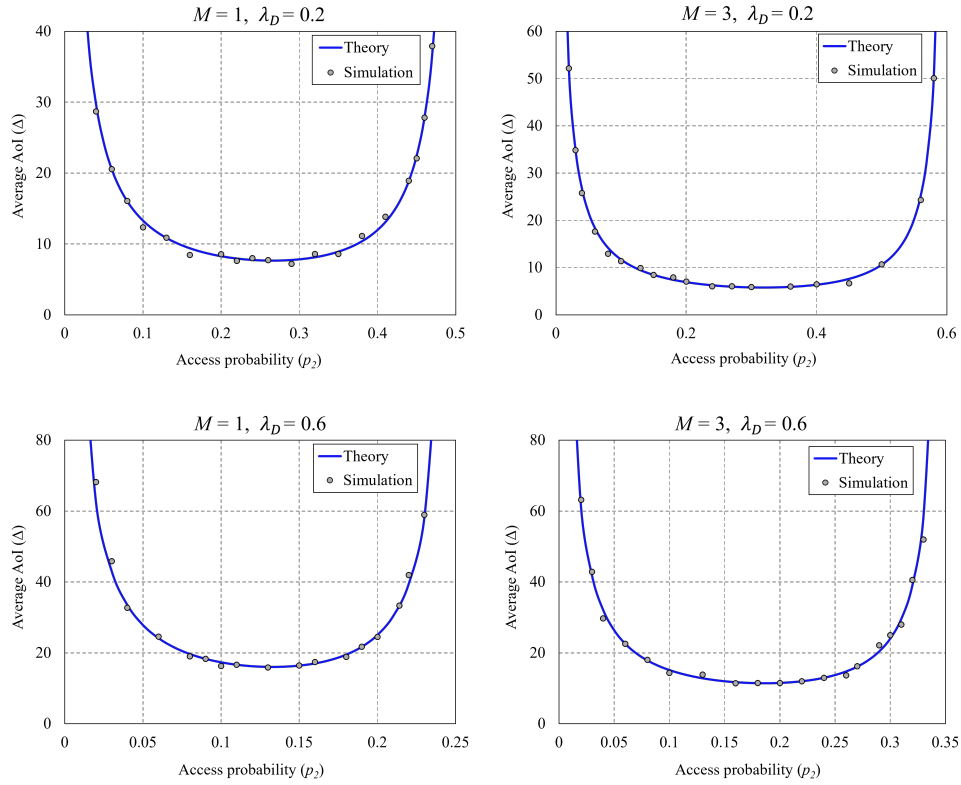


Fig. 5. The average AoI performance versus p_2 under different values of λ_D and M with $P_2 = 0.01$ mW.

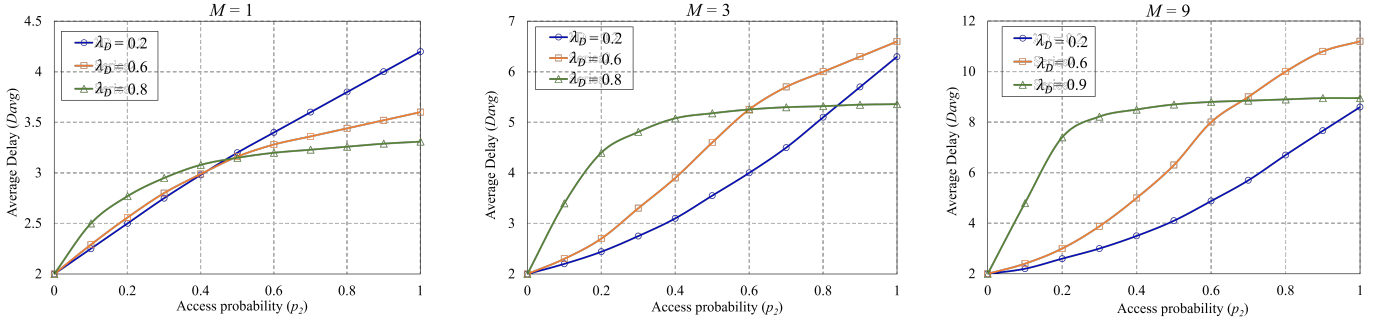


Fig. 6. The average delay performance versus p_2 under different values of λ_D and M with $P_2 = 0.01$ mW.

the optimal transmission power P_2^* are lower for higher λ_D in order to reduce the interference from the T_{AoI} nodes and satisfy D_{max} .

VII. CONCLUSION AND FUTURE WORK

In this paper, the inherent interplay between delay and AoI is investigated for a D2D-based heterogeneous IIoT network. We proposed a distributed backlog-aware access protocol and developed closed-form expressions for the average AoI and average delay using stochastic geometry and queuing theory. We evaluated the network performance using numerical results under different parameters and obtained optimal solutions that minimize the AoI via 2-D exhaustive numerical search. As a future work, this work can be extended to adopt queue man-

agement approaches and adaptive retransmission to introduce extra enhancement to the AoI. Moreover, we consider using machine learning-based techniques to set the optimal network parameters to adapt to the dynamic industrial environment.

ACKNOWLEDGEMENT

This paper has received funding from the European Union's Horizon 2020 research and innovation programme under grant agreement No. 883315.

APPENDIX

A. Proof of Proposition 1

The successful update probability p_{A_1} of an arbitrary T_{AoI} pair when the T_D node is active is given as

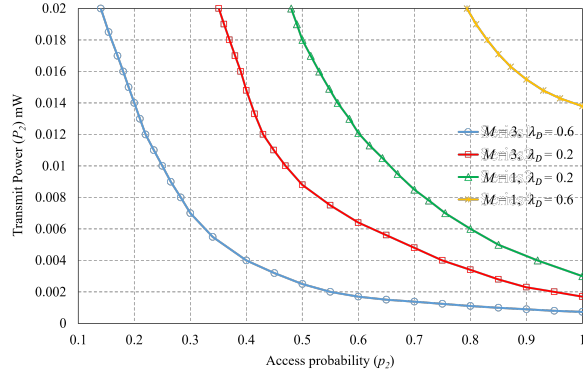


Fig. 7. The feasible region F_R under different values of λ_D and M .

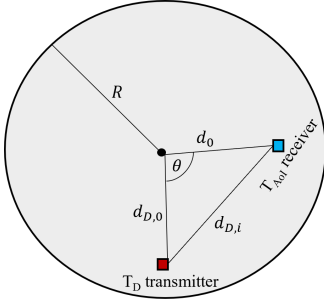


Fig. 8. Geometric representation of the distribution of the T_D transmitter and an arbitrary T_{AoI} receiver.

$$p_{A_1} = \Pr(\text{SINR}_i > \beta \mid \mathcal{K} = \phi_{A_1} \cup x_D) \\ = \Pr\left(\frac{P_2 |h_{i,i}|^2 d_A^\alpha}{\sigma^2 + \sum_{j \in \phi_{A_1} \setminus \{i\}} P_2 |h_{j,i}|^2 d_{j,i}^{-\alpha} + P_1 |h_{D,i}|^2 d_{D,i}^{-\alpha}} > \beta\right). \quad (27)$$

Since we have $|h_{i,i}|^2 \sim \exp(1)$ and $|h_{D,i}|^2 \sim \exp(1)$, so (27) can be rewritten as

$$p_{A_1} = \exp\left(-\frac{\beta \sigma^2 d_A^\alpha}{P_2}\right) \mathbb{E}\left[\int_0^\infty \exp\left(-\frac{P_1}{P_2} d_{D,i}^{-\alpha} x\right) e^{-x} dx\right] \\ \cdot \underbrace{\mathbb{E}\left[\exp\left(-s \sum_{j \in \phi_{A_1} \setminus \{i\}} |h_{j,i}|^2 d_{j,i}^{-\alpha}\right)\right]}_{L_S} \\ = \exp\left(-\frac{\beta \sigma^2 d_A^\alpha}{P_2}\right) \mathbb{E}\left[\frac{1}{1 + \frac{P_1}{P_2} \beta d_A^\alpha d_{D,i}^{-\alpha}}\right] \\ \cdot \underbrace{\mathbb{E}\left[\exp\left(-s \sum_{j \in \phi_{A_1} \setminus \{i\}} |h_{j,i}|^2 d_{j,i}^{-\alpha}\right)\right]}_{L_S}, \quad (28)$$

where the term L_S denotes the Laplace transform of the interference component of the nodes in ϕ_{A_1} which can be expressed as [44]

$$\mathbb{E}\left[\exp\left(-s \sum_{j \in \phi_{A_1} \setminus \{i\}} |h_{j,i}|^2 d_{j,i}^{-\alpha}\right)\right] = \exp\left[-\frac{\pi p_2 \lambda_A d_A^2 \beta^{\frac{2}{\alpha}}}{\text{sinc}(\frac{2}{\alpha})}\right]. \quad (29)$$

Based on [45], we can also have

$$\mathbb{E}\left[\frac{1}{1 + \frac{P_1}{P_2} \beta d_A^\alpha d_{D,i}^{-\alpha}}\right] \simeq \frac{1}{1 + \frac{d_A^2}{\mathbb{E}[d_{D,i}]^2} \left(\beta \frac{P_1}{P_2}\right)^{\frac{2}{\alpha}}}. \quad (30)$$

Then, with (29) and (30), p_{A_1} can be expressed as

$$p_{A_1} \simeq \exp\left[-\frac{\pi p_2 \lambda_A d_A^2 \beta^{\frac{2}{\alpha}}}{\text{sinc}(\frac{2}{\alpha})}\right] \frac{\exp\left(-\frac{\beta \sigma^2 d_A^\alpha}{P_2}\right)}{1 + \frac{d_A^2}{\mathbb{E}[d_{D,i}]^2} \left(\beta \frac{P_1}{P_2}\right)^{\frac{2}{\alpha}}} \quad (31)$$

The level of interference experienced by an arbitrary T_{AoI} receiver from the T_D transmitter depends on the distance $d_{D,i}$. Therefore, the term $\mathbb{E}[d_{D,i}]$ is calculated by taking the expectation over all the possible locations of that T_{AoI} receiver within the considered region \mathcal{C} . Since the locations of the T_{AoI} transmitters follow a homogeneous PPP model, we can consider that the locations of the T_{AoI} receivers approximately follow a uniform distribution in the region \mathcal{C} with a radius R . Accordingly, the distance d_0 of an arbitrary T_{AoI} receiver from origin of \mathcal{C} follow the probability distribution function $f_{d_0}(r)$ which is given by

$$f_{d_0}(r) = \begin{cases} \frac{2r}{R^2} & \text{if } 0 \leq r \leq R \\ 0 & \text{otherwise.} \end{cases} \quad (32)$$

If we consider the region \mathcal{C} depicted in Fig. 8, then we have

$$d_{D,i} = \sqrt{d_0^2 + d_{D,0}^2 - 2d_0 d_{D,0} \cos \theta}, \quad (33)$$

where $d_{D,0}$ is the distance from the T_D transmitter to the origin of the region \mathcal{C} , and $\theta \in \{0, 2\pi\}$ is a uniformly distributed random variable. Then, the expectation $\mathbb{E}[d_{D,i}]$ can be obtained as

$$\mathbb{E}[d_{D,i}] = \int_0^{2\pi} \frac{1}{2\pi} \int_0^R \frac{2r}{R^2} \sqrt{r^2 + d_{D,0}^2 - 2d_0 d_{D,0} \cos \theta} dr d\theta. \quad (34)$$

Based on (31) and (34), we can obtain the probability p_{A_1} , which concludes the proof.

B. Proof of Lemma 1

The balance equations for the DTMC in Fig. 3 can be obtained as

$$\lambda_D \pi_0 = (1 - \lambda_D) p_{D_1} \pi_1 \Leftrightarrow \pi_1 = \pi_0 \frac{\lambda_D}{(1 - \lambda_D) p_{D_1}} \\ \pi_1 (\lambda_D (1 - p_{D_1}) + (1 - \lambda_D) p_{D_1}) = \lambda_D \pi_0 + \pi_2 p_{D_1} (1 - \lambda_D) \\ \Leftrightarrow \pi_2 = \pi_0 \frac{\lambda_D^2 (1 - p_{D_1})}{(1 - \lambda_D)^2 p_{D_1}^2}. \quad (35)$$

Hence, for $1 \leq n \leq M$ we have

$$\pi_n = \frac{\lambda_D^n (1 - p_{D_1})^{(n-1)}}{p_{D_1}^n (1 - \lambda_D)^n} \pi_0, \quad (36)$$

while for $n > M$ we get

$$\pi_n = \frac{\lambda_D^n (1 - p_{D_1})^M (1 - p_{D_0})^{(n-M-1)}}{p_{D_1}^M p_{D_0}^{(n-M)} (1 - \lambda_D)^n} \pi_0 \quad (37)$$

Since we have $\sum_{n=0}^{\infty} \pi_n = 1$, with $\lambda_D \neq p_{D_1}$, the empty queue probability π_0 is expressed as

$$\pi_0 = \frac{(p_{D_1} - \lambda_D)(p_{D_0} - \lambda_D)}{p_{D_1} p_{D_0} - \lambda_D p_{D_1} - \lambda_D \left[\frac{\lambda_D(1-p_{D_1})}{(1-\lambda_D)p_{D_1}} \right]^M (p_{D_0} - p_{D_1})}. \quad (38)$$

When $\lambda_D = p_{D_1}$, (38) is no longer valid ($\pi_0 = \frac{0}{0}$). In this case we apply L'Hôpital's rule and get π_0 as

$$\pi_0 = \lim_{\lambda_D \rightarrow p_{D_1}} \frac{f'(\lambda_D)}{h'(\lambda_D)} = \frac{p_{D_0} - p_{D_1}}{p_{D_1} + (p_{D_0} - p_{D_1}) \frac{M+1-p_{D_1}}{1-p_{D_1}}}, \quad (39)$$

where $f(\lambda_D)$ and $h(\lambda_D)$ represent the nominator and denominator of (38), respectively. Combining (38) and (39), we get (16) which concludes the proof of *Lemma 1*.

C. Stability Condition of the T_{AOI} Node Queue

Our basic definition for the queue stability is based on Loynes' theorem [46]. The theorem states that, a queue is stable if the average service probability is greater than average arrival probability with the condition that the arrival process and the service process are strictly jointly stationary and. Hence, in order for the queue of the T_D to be stable, we need to prove that the DTMC in Fig. 3 irreducible Markov chain. Then, the average λ_D in (38) must satisfy the condition $0 < \pi_0 < 1$. We consider the following cases of the values of λ_D relative to the values of p_{D_1} and p_{D_0} :

- When $\lambda_D < p_{D_1} \Rightarrow \frac{\lambda_D(1-p_{D_1})}{(1-\lambda_D)p_{D_1}} < 1$, then $h(\lambda_D) > p_{D_0}(p_{D_1} - \lambda_D)$. Hence, we have $\pi_0 < \frac{p_{D_0} - \lambda_D}{p_{D_0}} = 1 - \frac{\lambda_D}{p_{D_0}} < 1$.
- When $\lambda_D = p_{D_1}$, based on (39), it is obvious that $0 < \pi_0 < 1$.
- When $p_{D_1} < \lambda_D < p_{D_0} \Rightarrow \frac{\lambda_D(1-p_{D_1})}{(1-\lambda_D)p_{D_1}} > 1$, then we have $f(\lambda_D) < 0$. Also, as from the following inequality

$$\begin{aligned} & \left(\frac{1 - \lambda_D}{1 - p_{D_1}} \right)^M \frac{p_{D_0} - \lambda_D}{p_{D_0} - p_{D_1}} < 1 < \left(\frac{\lambda_D}{p_{D_1}} \right)^{M+1} \\ & \Rightarrow p_{D_1}(p_{D_0} - \lambda_D) < \lambda_D \left(\frac{\lambda_D(1-p_{D_1})}{(1-\lambda_D)p_{D_1}} \right)^M (p_{D_0} - p_{D_1}) \\ & \Rightarrow h(\lambda_D) < 0. \end{aligned}$$

Thus, we have $\pi_0 = \frac{f(\lambda_D)}{h(\lambda_D)} > 0$. Since $\frac{\lambda_D(1-p_{D_1})}{(1-\lambda_D)p_{D_1}} > 1$, we also have $h(\lambda_D) < p_{D_0}(p_{D_1} - \lambda_D) < 0$, so we obtain $\pi_0 < 1 - \frac{\lambda_D}{p_{D_0}} < 1$

From the discussion of the above cases, we can see that the condition $0 < \pi_0 < 1$ is verified, and we can conclude that the queue of T_D node is stable if $\lambda_D < p_{D_0}$.

D. Proof of Lemma 2

The probability $\Pr(1 \leq Q \leq M)$ is obtained as

$$\Pr(1 \leq Q \leq M) = \sum_{n=1}^M \pi_n. \quad (40)$$

Based on (15) and when $\lambda_D < p_{D_0}$ and $\psi \neq 1$, we get

$$\begin{aligned} \Pr(1 \leq Q \leq M) &= \frac{\pi_0}{1 - p_{D_1}} \sum_{n=1}^M \left(\frac{\lambda_D(1-p_{D_1})}{(1-\lambda_D)p_{D_1}} \right)^n \\ &= \frac{\pi_0}{1 - p_{D_1}} \frac{\frac{\lambda_D(1-p_{D_1})}{(1-\lambda_D)p_{D_1}} - \left(\frac{\lambda_D(1-p_{D_1})}{(1-\lambda_D)p_{D_1}} \right)^{n+1}}{1 - \frac{\lambda_D(1-p_{D_1})}{(1-\lambda_D)p_{D_1}}} \\ &= \frac{\pi_0 \lambda_D (1 - \psi^M)}{p_{D_1} - \lambda_D} \\ &= \frac{\lambda_D (1 - \psi^M) (p_{D_0} - \lambda_D)}{p_{D_1} p_{D_0} - \lambda_D p_{D_1} - \lambda_D \psi^M (p_{D_0} - p_{D_1})}. \end{aligned} \quad (41)$$

For $n > M$, we obtain $\Pr(Q > M)$ as

$$\begin{aligned} \Pr(Q > M) &= \sum_{n=M+1}^{\infty} \pi_n = 1 - \pi_0 - \sum_{n=1}^M \pi_n \\ &= \frac{\lambda_D \psi^M (p_{D_1} - \lambda_D)}{p_{D_1} p_{D_0} - \lambda_D p_{D_1} - \lambda_D \psi^M (p_{D_0} - p_{D_1})}. \end{aligned} \quad (42)$$

E. Proof of Theorem 1

The average queue size Q_{avg} of the T_{AOI} node can be given as

$$\begin{aligned} Q_{avg} &= \sum_{n=1}^{\infty} n \pi_n = \sum_{n=1}^M n \pi_n + \sum_{n=M+1}^{\infty} n \pi_n \\ &= \sum_{n=1}^M n \pi_n + \sum_{n=1}^{\infty} (M+n) \pi_{M+n} \\ &= \underbrace{\sum_{n=1}^M n \pi_n}_{R_1} + \underbrace{M \sum_{n=1}^{\infty} \pi_{M+n}}_{R_2} + \underbrace{\sum_{n=1}^{\infty} n \pi_{M+n}}_{R_3} \end{aligned} \quad (43)$$

With $\lambda_D < p_{D_0}$ and $\psi \neq 1$, the first term R_1 can be obtained as

$$\begin{aligned}
\sum_{n=1}^M n\pi_n &= \sum_{n=1}^M n \frac{\lambda_D^n (1-p_{D_1})^{(n-1)}}{p_{D_1}^n (1-\lambda_D)^n} \pi_0 \\
&= \frac{\pi_0 \lambda_D}{(1-\lambda_D)p_{D_1}} \sum_{n=1}^M n \left[\frac{\lambda_D (1-p_{D_1})}{p_{D_1} (1-\lambda_D)} \right]^{(n-1)} \\
&= \frac{\pi_0 \lambda_D}{(1-\lambda_D)p_{D_1}} \left(\sum_{n=1}^M \left[\frac{\lambda_D (1-p_{D_1})}{p_{D_1} (1-\lambda_D)} \right]^n \right)' \\
&= \frac{\pi_0 \lambda_D}{(1-\lambda_D)p_{D_1}} \frac{M\psi^{(M+1)} - \psi^M (M+1) + 1}{\left(1 - \frac{\lambda_D (1-p_{D_1})}{p_{D_1} (1-\lambda_D)}\right)^2} \\
&= \frac{\lambda_D (1-\lambda_D)p_{D_1} \frac{p_{D_0}-\lambda_D}{p_{D_1}-\lambda_D} (M\psi^{(M+1)} - \psi^M (M+1) + 1)}{p_{D_1}p_{D_0} - \lambda_D p_{D_1} - \lambda_D \psi^M (p_{D_0} - p_{D_1})} \quad (44)
\end{aligned}$$

Based on the results of (18), the term R_2 is obtained as

$$\begin{aligned}
M \sum_{n=1}^{\infty} \pi_{M+n} &= M \Pr(Q > M) \\
&= \frac{\lambda_D \psi^M (p_{D_1} - \lambda_D)}{p_{D_1}p_{D_0} - \lambda_D p_{D_1} - \lambda_D \psi^M (p_{D_0} - p_{D_1})} \quad (45)
\end{aligned}$$

Finally, the term R_3 can be obtained using the results from (37)

$$\begin{aligned}
\sum_{n=1}^{\infty} n\pi_{M+n} &= \frac{\pi_0 \lambda_D \psi^M}{p_{D_0} (1-\lambda_D)} \sum_{n=1}^{\infty} n \left[\frac{\lambda_D (1-p_{D_0})}{p_{D_0} (1-\lambda_D)} \right]^{(n-1)} \\
&= \frac{\pi_0 \lambda_D \psi^M}{p_{D_0} (1-\lambda_D)} \frac{1}{\left(1 - \frac{\lambda_D (1-p_{D_0})}{p_{D_0} (1-\lambda_D)}\right)^2} \\
&= \frac{\lambda_D (1-\lambda_D)p_{D_0} \psi^M \frac{p_{D_1}-\lambda_D}{p_{D_0}-\lambda_D}}{p_{D_1}p_{D_0} - \lambda_D p_{D_1} - \lambda_D \psi^M (p_{D_0} - p_{D_1})} \quad (46)
\end{aligned}$$

Substituting (44), (45) and (46) in (43), we get

$$Q_{avg} = \frac{Q_1 + Q_2}{p_{D_0}p_{D_1} - \lambda_D p_{D_1} - \lambda_D \psi^M (p_{D_0} - p_{D_1})}, \quad (47)$$

where we have

$$\begin{aligned}
Q_1 &= \lambda_D (1-\lambda_D) p_{D_1} \frac{p_{D_0}-\lambda_D}{p_{D_1}-\lambda_D} \\
&\quad \cdot (M\psi^{(M+1)} - \psi^M (M+1) + 1), \\
Q_2 &= \psi^M \lambda_D (p_{D_1} - \lambda_D) \left(M + \frac{p_{D_0} (1-\lambda_D)}{p_{D_0} - \lambda_D} \right). \quad (48)
\end{aligned}$$

REFERENCES

- [1] J. Lin, W. Yu, N. Zhang, X. Yang, H. Zhang, and W. Zhao, "A survey on internet of things: Architecture, enabling technologies, security and privacy, and applications," *IEEE Internet of Things Journal*, vol. 4, no. 5, pp. 1125–1142, 2017.
- [2] G. Intelligence. (2021) The mobile economy 2021. [Online]. Available: <https://www.gsma.com/mobileeconomy/>
- [3] E. Sisinni, A. Saifullah, S. Han, U. Jennehag, and M. Gidlund, "Industrial internet of things: Challenges, opportunities, and directions," *IEEE Transactions on Industrial Informatics*, vol. 14, no. 11, pp. 4724–4734, 2018.
- [4] F. Ademaj, M. Rzymowski, H.-P. Bernhard, K. Nyka, and L. Kulas, "Relay-aided wireless sensor network discovery algorithm for dense industrial iot utilizing espar antennas," *IEEE Internet of Things Journal*, vol. 8, no. 22, pp. 16 653–16 665, 2021.
- [5] L. Liu and W. Yu, "A d2d-based protocol for ultra-reliable wireless communications for industrial automation," *IEEE Transactions on Wireless Communications*, vol. 17, no. 8, pp. 5045–5058, 2018.
- [6] H. Farag, E. Sisinni, M. Gidlund, and P. Österberg, "Priority-aware wireless fieldbus protocol for mixed-criticality industrial wireless sensor networks," *IEEE Sensors Journal*, vol. 19, no. 7, pp. 2767–2780, 2019.
- [7] M. Li, C. Chen, C. Hua, and X. Guan, "Learning-based autonomous scheduling for aoi-aware industrial wireless networks," *IEEE Internet of Things Journal*, vol. 7, no. 9, pp. 9175–9188, 2020.
- [8] P. Gil, A. Santos, and A. Cardoso, "Dealing with outliers in wireless sensor networks: An oil refinery application," *IEEE Transactions on Control Systems Technology*, vol. 22, no. 4, pp. 1589–1596, 2014.
- [9] Y. Sun, E. Uysal-Biyikoglu, R. D. Yates, C. E. Koksal, and N. B. Shroff, "Update or wait: How to keep your data fresh," *IEEE Transactions on Information Theory*, vol. 63, no. 11, pp. 7492–7508, 2017.
- [10] R. Li, P. Hong, K. Xue, M. Zhang, and T. Yang, "Resource allocation for uplink noma-based d2d communication in energy harvesting scenario: A two-stage game approach," *IEEE Transactions on Wireless Communications*, vol. 21, no. 2, pp. 976–990, 2022.
- [11] H. H. Yang, C. Xu, X. Wang, D. Feng, and T. Q. S. Quek, "Understanding age of information in large-scale wireless networks," *IEEE Transactions on Wireless Communications*, vol. 20, no. 5, pp. 3196–3210, 2021.
- [12] R. D. Yates, "The age of information in networks: Moments, distributions, and sampling," *IEEE Transactions on Information Theory*, vol. 66, no. 9, pp. 5712–5728, 2020.
- [13] M. Costa, M. Codreanu, and A. Ephremides, "On the age of information in status update systems with packet management," *IEEE Transactions on Information Theory*, vol. 62, no. 4, pp. 1897–1910, 2016.
- [14] A. Kosta, N. Pappas, A. Ephremides, and V. Angelakis, "Age of information performance of multiaccess strategies with packet management," *Journal of Communications and Networks*, vol. 21, no. 3, pp. 244–255, 2019.
- [15] C. Kam, S. Kompella, G. D. Nguyen, J. E. Wieselthier, and A. Ephremides, "On the age of information with packet deadlines," *IEEE Transactions on Information Theory*, vol. 64, no. 9, pp. 6419–6428, 2018.
- [16] I. Kadota, A. Sinha, E. Uysal-Biyikoglu, R. Singh, and E. Modiano, "Scheduling policies for minimizing age of information in broadcast wireless networks," *IEEE/ACM Transactions on Networking*, vol. 26, no. 6, pp. 2637–2650, 2018.
- [17] R. Talak, S. Karaman, and E. Modiano, "Improving age of information in wireless networks with perfect channel state information," *IEEE/ACM Transactions on Networking*, vol. 28, no. 4, pp. 1765–1778, 2020.
- [18] C. Li, Q. Liu, S. Li, Y. Chen, Y. T. Hou, W. Lou, and S. Kompella, "Scheduling with age of information guarantee," *IEEE/ACM Transactions on Networking*, pp. 1–14, 2022.
- [19] H. Farag, M. Gidlund, and Č. Stefanović, "A deep reinforcement learning approach for improving age of information in mission-critical iot," in *2021 IEEE Global Conference on Artificial Intelligence and Internet of Things (GCAIoT)*, 2021, pp. 14–18.
- [20] M. Elnourani, S. Deshmukh, and B. Beferull-Lozano, "Distributed resource allocation in underlay multicast d2d communications," *IEEE Transactions on Communications*, vol. 69, no. 5, pp. 3409–3422, 2021.
- [21] G. Chisci, H. Elsayy, A. Conti, M.-S. Alouini, and M. Z. Win, "Uncoordinated massive wireless networks: Spatiotemporal models and multiaccess strategies," *IEEE/ACM Transactions on Networking*, vol. 27, no. 3, pp. 918–931, 2019.
- [22] M. Liu and L. Zhang, "Resource allocation for d2d underlay communications with proportional fairness using iterative-based approach," *IEEE Access*, vol. 8, pp. 143 787–143 801, 2020.
- [23] P. D. Mankar, M. A. Abd-Elmagid, and H. S. Dhillon, "Spatial distribution of the mean peak age of information in wireless networks," *IEEE Transactions on Wireless Communications*, vol. 20, no. 7, pp. 4465–4479, 2021.

- [24] H. H. Yang, A. Arafa, T. Q. S. Quek, and H. V. Poor, "Optimizing information freshness in wireless networks: A stochastic geometry approach," *IEEE Transactions on Mobile Computing*, vol. 20, no. 6, pp. 2269–2280, 2021.
- [25] J. Li, D. Wu, C. Yue, Y. Yang, M. Wang, and F. Yuan, "Energy-efficient transmit probability-power control for covert d2d communications with age of information constraints," *IEEE Transactions on Vehicular Technology*, pp. 1–15, 2022.
- [26] M. Li, C. Chen, H. Wu, X. Guan, and X. Shen, "Age-of-information aware scheduling for edge-assisted industrial wireless networks," *IEEE Transactions on Industrial Informatics*, vol. 17, no. 8, pp. 5562–5571, 2021.
- [27] I. Kadota, A. Sinha, and E. Modiano, "Scheduling algorithms for optimizing age of information in wireless networks with throughput constraints," *IEEE/ACM Transactions on Networking*, vol. 27, no. 4, pp. 1359–1372, 2019.
- [28] J. Sun, L. Wang, Z. Jiang, S. Zhou, and Z. Niu, "Age-optimal scheduling for heterogeneous traffic with timely throughput constraints," *IEEE Journal on Selected Areas in Communications*, vol. 39, no. 5, pp. 1485–1498, 2021.
- [29] L. Luo, Z. Liu, Z. Chen, M. Hua, W. Li, and B. Xia, "Age of information-based scheduling for wireless d2d systems with a deep learning approach," *IEEE Transactions on Green Communications and Networking*, pp. 1–1, 2022.
- [30] A. M. Bedewy, Y. Sun, and N. B. Shroff, "Minimizing the age of information through queues," *IEEE Transactions on Information Theory*, vol. 65, no. 8, pp. 5215–5232, 2019.
- [31] R. Talak and E. H. Modiano, "Age-delay tradeoffs in queueing systems," *IEEE Transactions on Information Theory*, vol. 67, no. 3, pp. 1743–1758, 2021.
- [32] R. Devassy, G. Durisi, G. C. Ferrante, O. Simeone, and E. Uysal, "Reliable transmission of short packets through queues and noisy channels under latency and peak-age violation guarantees," *IEEE Journal on Selected Areas in Communications*, vol. 37, no. 4, pp. 721–734, 2019.
- [33] P. Park, S. Coleri Ergen, C. Fischione, C. Lu, and K. H. Johansson, "Wireless network design for control systems: A survey," *IEEE Communications Surveys Tutorials*, vol. 20, no. 2, pp. 978–1013, 2018.
- [34] R. Talak, S. Karaman, and E. Modiano, "Optimizing age of information in wireless networks with perfect channel state information," in *2018 16th International Symposium on Modeling and Optimization in Mobile, Ad Hoc, and Wireless Networks (WiOpt)*, 2018, pp. 1–8.
- [35] M. Haenggi, *Geometry for Wireless Networks*. Cambridge, UK: Cambridge Univ. Press, 2012.
- [36] E. T. Ceran, D. Gündüz, and A. György, "Average age of information with hybrid arq under a resource constraint," *IEEE Transactions on Wireless Communications*, vol. 18, no. 3, pp. 1900–1913, 2019.
- [37] I. Kadota, A. Sinha, E. Uysal-Biyikoglu, R. Singh, and E. Modiano, "Scheduling policies for minimizing age of information in broadcast wireless networks," *IEEE/ACM Transactions on Networking*, vol. 26, no. 6, pp. 2637–2650, 2018.
- [38] B. Sombabu and S. Moharir, "Age-of-information based scheduling for multi-channel systems," *IEEE Transactions on Wireless Communications*, vol. 19, no. 7, pp. 4439–4448, 2020.
- [39] M. Zorzi and R. Rao, "Capture and retransmission control in mobile radio," *IEEE Journal on Selected Areas in Communications*, vol. 12, no. 8, pp. 1289–1298, 1994.
- [40] L. Kleinrock, *Queueing Systems, Volume 1: Theory*. London, UK: Wiley-Interscience, 1975.
- [41] D. P. Bertsekas and R. G. Gallager, *Data Networks*. NJ, USA: Prentice-Hall, 1992.
- [42] M. Haenggi, *Stochastic Geometry for Wireless Networks*. Cambridge, UK: Cambridge Univ. Press, 2012.
- [43] I. Griva, S. Nash, and A. Sofer, *Linear and Nonlinear Optimization*. Cambridge, UK: Cambridge Univ. Press, 2009.
- [44] M. Haenggi and R. K. Ganti, *Interference in Large Wireless Networks*. Boston, USA: Now Foundations and Trends, 2009.
- [45] N. Lee, X. Lin, J. G. Andrews, and R. W. Heath, "Power control for d2d underlaid cellular networks: Modeling, algorithms, and analysis," *IEEE Journal on Selected Areas in Communications*, vol. 33, no. 1, pp. 1–13, 2015.
- [46] R. M. Loynes, "The stability of a queue with non-independent interarrival and service times," *Math. Proc. Cambridge Philos. Soc.*, vol. 58, no. 3, p. 497–520, 1962.